Arabian Journal of Chemistry (2020) 13, 7212–7223

King Saud University

Arabian Journal of Chemistry

www.ksu.edu.sa
www.sciencedirect.com

ORIGINAL ARTICLE

The starch modified montmorillonite for the removal of Pb(II), Cd(II) and Ni(II) ions from aqueous solutions

Hung Nguyen Van [a,b], Hai Chu Van [b], Tam Luu Hoang [c,e], Dang Khoa Vo Nguyen [a], Chi Nhan Ha Thuc [d,e,*]

[a] *Graduate University of Science and Technology, VAST – Viet Nam Academy of Science and Technology, Viet Nam*
[b] *Center of Analytical Service and Experiment, HCMC, Viet Nam*
[c] *Materials Technology Faculty, University of Technology, VNU-HCM, Viet Nam*
[d] *Faculty of Materials Science and Technology, University of Science, VNU-HCM, Viet Nam*
[e] *Vietnam National University, Ho Chi Minh City, Viet Nam*

Received 19 April 2020; accepted 2 August 2020
Available online 10 August 2020

KEYWORDS

Adsorbent;
Montmorillonite/starch;
Isotherm adsorption

Abstract In the present study, we attempted to synthesize a novel sorbent from the starch modified montmorillonite for the removal of Pb(II), Cd(II), and Ni(II) ions from aqueous solutions. Structure and properties of the adsorbent were characterized by Fourier-transformed infrared(FT-IR) spectroscopy, X-ray diffraction (XRD), and Field emission scanning electron microscopic (FE-SEM) techniques. Batch experiments were confirmed through the effect of different conditions including pH, contact time, initial metal concentration and adsorbent dose. Specifically, the optimum value of adsorbent dose was achieved as 20 g/l for the removal of almost metal ions. The adsorption data was fitted with the optimum pH value as 5 for all experiments. The contact time at which the uptake of maximum metal adsorption was observed within 45 min for Pb(II), 90 min for Cd(II), and 60 min for Ni(II). In addition, it was revealed in our study that the equilibrium data obeyed the Langmuir model, and the adsorption kinetic followed a pseudo second-order rate model. Obtained results were noticeable for a modified phyllosilicate adsorbent, and with such a simple and low-cost modification for montmorillonite, the potential of this material as an economical and effective adsorbent for the removal of metal ions from aqueous solution was considerably elevated.

* Corresponding author at: Faculty of Materials Science and Technology, University of Science, VNU-HCM, Viet Nam.
E-mail addresses: hoangtam@hcmut.edu.vn (T. Luu Hoang), htcnhan@hcmus.edu.vn (C.N. Ha Thuc).
Peer review under responsibility of King Saud University.

Production and hosting by Elsevier

https://doi.org/10.1016/j.arabjc.2020.08.003
1878-5352

1. Introduction

In developing countries (Namasivayam and Sangeetha, 2006), heavy metals contamination, from both industrial and agricultural activities, has been a serious threat to human, wildlife, and the quality of natural water sources (Tian et al., 2011, Masoumi et al., 2016, Kenawy et al., 2017). Such activities released a lot of highly toxic heavy metals such as lead, cadmium, nickel, mercury and chromium, which do harm to the liver, kidney, nervous system, brain cells, hematopoietic, and productive systems (Mousavi et al., 2018, Luo et al., 2015, Hu et al., 2018, Achazhiyath Edathil et al., 2018). Because heavy metal contaminants are not biodegradable and decomposable (Mende et al., 2016, Rathinam et al., 2018, Bo et al., 2018, Dimpe et al., 2018), the World Health Organization (WHO) recommended extremely low maximum acceptable concentration for cadmium, lead, nickel and chromium contamination in drinking water, with values of 0.003 mg/L, 0.01 mg/L, 0.02 mg/L and 0.05 mg/L, respectively (Oninla et al., 2018). In order to diminish the remaining amount of these harmful metals in aqueous solutions to a safe level for human and the environment, several methods of adsorption such as: electrochemical treatment, chemical precipitation, reverse osmosis, evaporation, filtration, oxidation, ion exchange, coagulation, and membrane separation have been successfully employed (Dardouri et al., 2018, Sun et al., 2018, Tohdee et al., 2018, Semerjian, 2018, Li et al., 2019, Fakhre and Ibrahim, 2018). Among these techniques, adsorption is widely applied for industrial water because of its low-cost, easy operation, and high efficiency for removing heavy metal from aqueous solution (Dai et al., 2018). In previous studies, different adsorbents have been investigated such as active carbon, silica, natural adsorbents, clay material, zeolites, sugarcane bagasse, rice husk, loofah, coffee grounds, chitosan, cellulose, rice straw etc. (Sandoval et al., 2018, Sellaoui et al., 2018, Dong et al., 2016, Rytwo et al., 2007, Li et al., 2018, Akpomie and Dawodu, 2016, Eeshwarasinghe et al., 2019, Karri et al., 2020, Chuah et al., 2005, Tang et al., 2014). Out of studied adsorbents, montmorillonite emerged as a reasonable one to be applied, especially in Vietnam, thanks to its abundance in some regions (Thuc et al., 2010). Moreover, modified montmorillonite has been revealed to exhibit higher adsorbing capability than the primitive one (Huang et al., 2020), so it was preferred to be applied in toxic metals elimination in aqueous solutions. In this study, the montmorillonite was denatured by Vietnamese cassava starch, a common and low-cost modifier, to form an adsorbent material for Pb(II), Cd(II), and Ni (II) ions, three typical heavy metal ions, removal from aqueous solutions. The effect of solution pH, dose, initial concentration and contact time during the process were also investigated. The batch experiments were determined the parameter associated of Langmuir, Freundlich, Redlich-Peterson and Sips isotherms.

2. Experimental

2.1. Reagents and material

Montmorillonite (purity > 95%) (MMT) was purified from raw bentonite in Lam Dong Province, Vietnam. Cassava starch (amylose pectin content > 80% wt). Lead(II) nitrate, cadmium(II) nitrate, and nickel(II) nitrate were purchased from Merck (Germany). The standard solutions of (1000 mg/L) diluted nitric acid (1%) to prepare several aqueous solutions of desired concentrations (40–400 mg/L).

2.2. Preparation of pure montmorillonite

5 g of raw bentonite was added to 250 mL of distilled water and stirred for 24 h. The solution was transferred to a column (diameter of 15 cm and height of 1 m) for 12 h. After settling, the bottom precipitation was removed and the refined montmorillonite (labeled as MMT) was centrifuged at 9000 rpm and dried at 50 °C for 24 h.

2.3. Synthesis of the adsorbent

The modification of MMT by starch has been followed the methods as reported in our previous study (Tam et al., 2019). The starch was stirred in 50 mL of distilled water at 50 °C for 30 min. 4 g of MMT was stirred in 250 mL of distilled water for 24 h. The starch solution was then added in MMT suspension with the mass ratio of MMT/Starch(1/0.6), and the mixture was continuously stirred at room temperature during 2 h. The modified MMT (MMT/starch) was centrifuged at 9000 rpm and washed three times with distilled water. The sample was finally dried at 50 °C for 24 h and sieved to obtain the particle size of below 200 μm. The adsorbent was stored in a desiccator for the removal of Pb(II), Cd (II), and Ni(II) ions from aqueous solutions.

2.4. Characterization

The morphologies of MMT/Starch was observed by Field emission scanning electron microscopic – Energy dispersive X-ray spectroscopy (FE-SEM/EDX, Hitachi S-4800, Japan). The modified material was measured in range of 400–4000 cm^{-1} by using Nicolet iS 50 Fourier-transformed infrared spectroscopy (FT-IR, Thermo, USA) and the point zero charge was determinated by pH meter (JENWAY) at room temperature. The thermogravimetric analyzer (TGA 55, USA) was used to measure the sample stability with heating speed of 20 °C/min from 38 to 900 °C. The analytical tool of Brunauer-Emmett-Teller (BET, A Quantachrome Autosorb iQ2) was determinated the surface area of the modified adsorbent. The pH of initial solutions were used to analyze the point of zero charge (PZC) of MMT/Starch adsorbent based on the drift process (Kosmulski, 2009). Approximately 0.1 g of MMT/Starch was put into 50 mL of NaCl 0.1 M solution each 100 mL Erlenmeyer flask and the initial pH was adjusted from pH 3 to 12 by adding HCl 1 M or NaOH 1 M (Tran et al., 2017). The flasks were sealed and shaked at 150 rpm in 24 h, which were centrifuged to obtain solution of final pH (pH_f). In essence, the difference of solutions at the value of pH_i and pH_f were plotted to pH_i, the intersection point of the ΔpH curve with pH_i was performed at pH_{zpc}.

2.5. Adsorption experiments

The dose of MMT/Starch (0.2–1.2 g) was carried out by immersing the adsorbent into 50 mL of the Pb(II), Cd(II), and Ni(II) ions at pH of 4–6 and different initial concentra-

tions (40–400 mg/L) under constant agitation. All batch experiments were shaken with a constant speed at 150 rpm in a shaker at room temperature, the mixture was centrifuged at 9000 rpm for 10 min. The remaining concentration of Pb(II), Cd(II), and Ni(II) ions weremeasured by an Inductively Coupled Plasma Optical Emission Spectrometry (ICP-OES, PerkinElmer, Optima 8300). The adsorption capacities at equilibrium (q_e, mg/g) was calculated by the following equations:

$$q_e = \frac{(C_o - C_e)xV}{m} \quad (1)$$

Where C_o and C_e are the initial concentration (mg/L) and the equilibrium concentration (mg/L), V is the volume of the solution (L), and m is the mass of MMT/starch (g). In order to determine the characteristics of kinetic models and equilibrium adsorption of Pb(II), Cd(II), Ni(II) ions. The experimental process were investigated by using the 1.0 g of adsorbent in the range from 40 to 400 mg/L with different shaking periods from 1 to 120 min.

3. Results and discussion

3.1. Characterization of MMT/Starch

FTIR spectra (Fig. 1a) of MMT showed a peak of OH stretching band at 3303 cm^{-1} and a peak of OH stretching vibration at 1635 cm^{-1} (Lozano-Morales et al., 2018). Besides, the spectra of MMT/Starch appeared a broad peak of OH group at 3424 cm^{-1}, and the peaks at 1420 cm^{-1} and 997 cm^{-1} can be elucidated as the stretch vibration of C-O band in the functional groups of C-O-H and C-O-C in the starch, respectively (Majdzadeh-Ardakani et al., 2010). Those results indicated the load of starch molecules into the layers of MMT.

Fig. 1b showed the diffraction patterns of the MMT and the MMT/Starch. The d_{001} of diffraction peak of MMT at 9° (2θ) and the MMT/Starch shifted to a lower angle of 5° from the pure MMT. It can be inferred from these results that the loading starch entered MMT and the structure of MMT/Starch adsorbent was obtained MMT and Starch.

The morphology of MMT, Starch and MMT/Starch were shown in Fig. 2, with the image of starch showed homogeneous particle with an average size of 20 μm. Meanwhile, the surface of MMT/Starch particles were in spherical shape, with clear geometric boundaries. In addition, the elemental analysis of MMT/Starch was indicated in Fig. 2d. The result table presented that the adsorbent composition including C, O, Na, Al, Si, K, Ca, and Fe with 30.4 wt%, 49.2 wt%, 0.7 wt%, 3.4 wt%, 11.2 wt%, 1.5 wt%, 2.2 wt%, and 1.4 wt%, respectively.

Fig. 3a indicated TGA curves in the range 38–900 °C at a speed rate of 20 °C/min under nitrogen flow. The results of mass loss had thoroughly ocurred three stages, the first stage was removed the adsorbed water and the degradation of starch (< 250 °C). In the second phase of the temperature range of 250–350 °C, the loss mass of Starch and MMT/starch were decreased sharply 82.2% and 44,7%, respectively. On the other hand, the loss mass of MMT was reduced slightly about 3% in range 250–350 °C. As a result, starch was grafted into the structure of MMT. The final stage was decreased slightly the weight loss between the temperatures 350–650 °C, which attributed in the destruction of complete structure including MMT/Starch, MMT, and Starch. After 650 °C, the process of degradation was obtained the residual compositions and no mass change destruction of complete structure.

As a result of the Brunanuer-Emmett-Teller (BET) analysis, the nitrogen isotherm of desorption-adsorption was calculated at a temperature of 77 K with N_2 using A Quantachrome Autosorb iQ2 analysis indicating the type I adsorption isotherm and characteristic adsorbent. Moreover, the results was shown that the measured values of pore volume, pore width, and surface area with 0.028 (cc/g), 3.627 nm, and 12.988 m^2/g were reported in Fig. 3b.

3.2. Influencing factors of metal ions adsorption

3.2.1. Influence of solution pH

In essence, the removal capacity of adsorbent depends on the pH value of solution, which is an important factor of the adsorption process because it affects the active sites of function groups and the surface of the adsorbent. As a result in Fig. 4a,

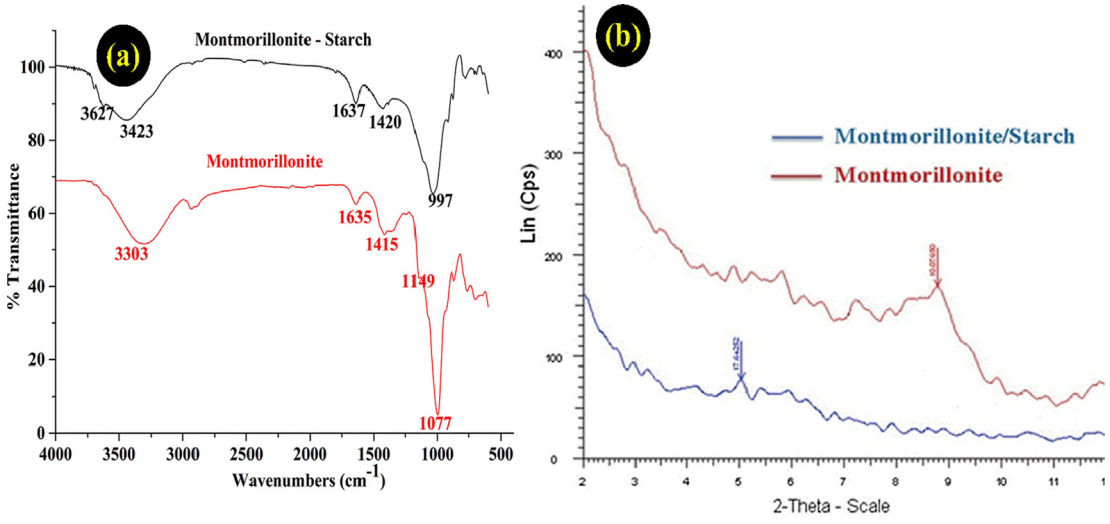

Fig. 1 FT-IR spectra (a) and XRD patterns (b) of montmorillonite and montmorillonite/Starch.

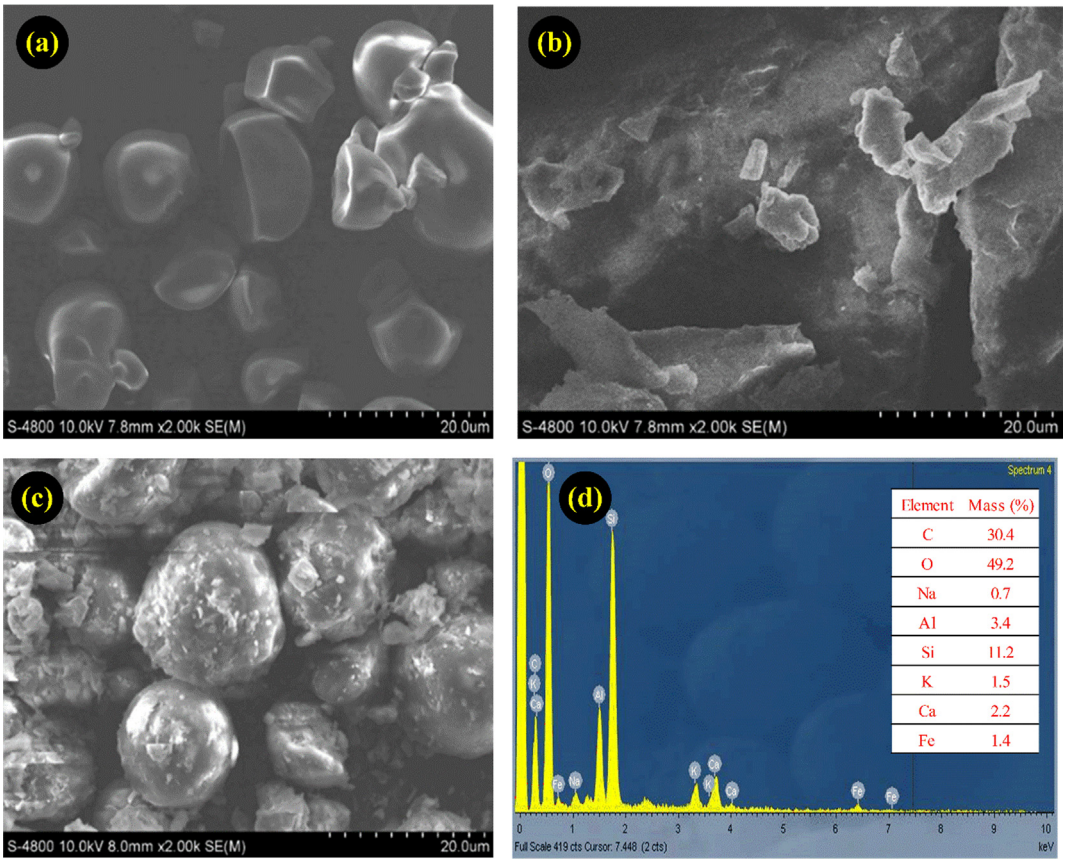

Fig. 2 SEM images of Starch (a), MMT (b), MMT/Starch adsorbent (c), and elemental analysis spectra of MMT/Starch (d).

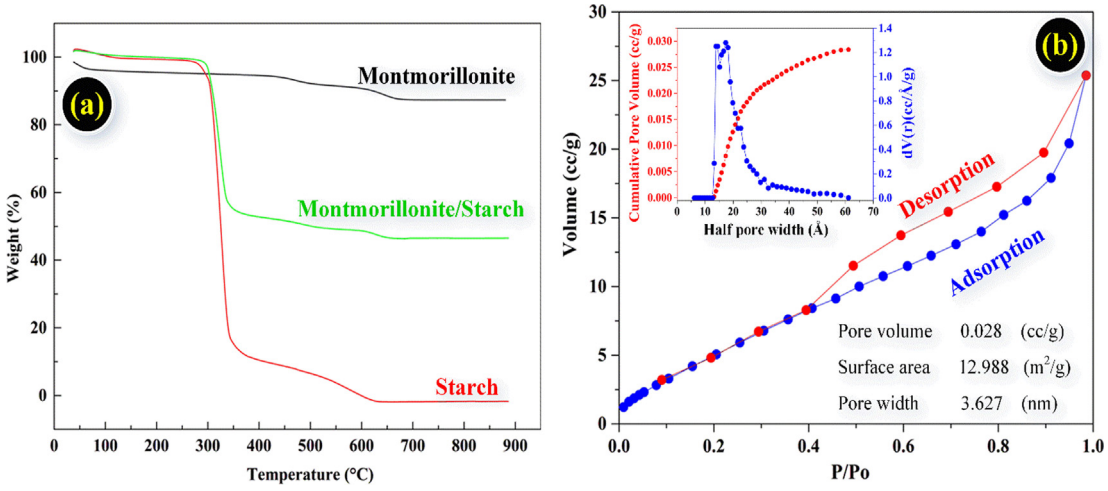

Fig. 3 The TGA characterization studies of Montmorillonite, Starch, MMT/Starch (a), the adsorption/desorption isotherm onto MMT/Starch at 77 K and the calculated results of adsorbent (b).

the pH_{zpc} of MMT/Starch was 8.8. Therefore, MMT/Starch become a positively charged adsorbent on the surface when the solution of pH was lower than the pH_{zpc} value. Consequently, the charged surface obtained a negatively adsorbent when the pH value was higher than the pH_{pzc} factor (8.8). However, the pH of all solutions in Fig. 4b investigated in the range of 4–6. The adsorption capacity related to the active sites of the adsorbent and the metal ions. At low pH values, the strong competition occurred between H^+ and metal ions in the solution, which decreased the uptake of metal ions at the active positions. On the other hand, when the pH value is higher than the precipitation of the metal ions (pH > 6), the removal rate was not calculated. In addition, the adsorption uptake of Pb (II), Cd(II), and Ni(II) increased from 97.5% to 99%, 94.7%

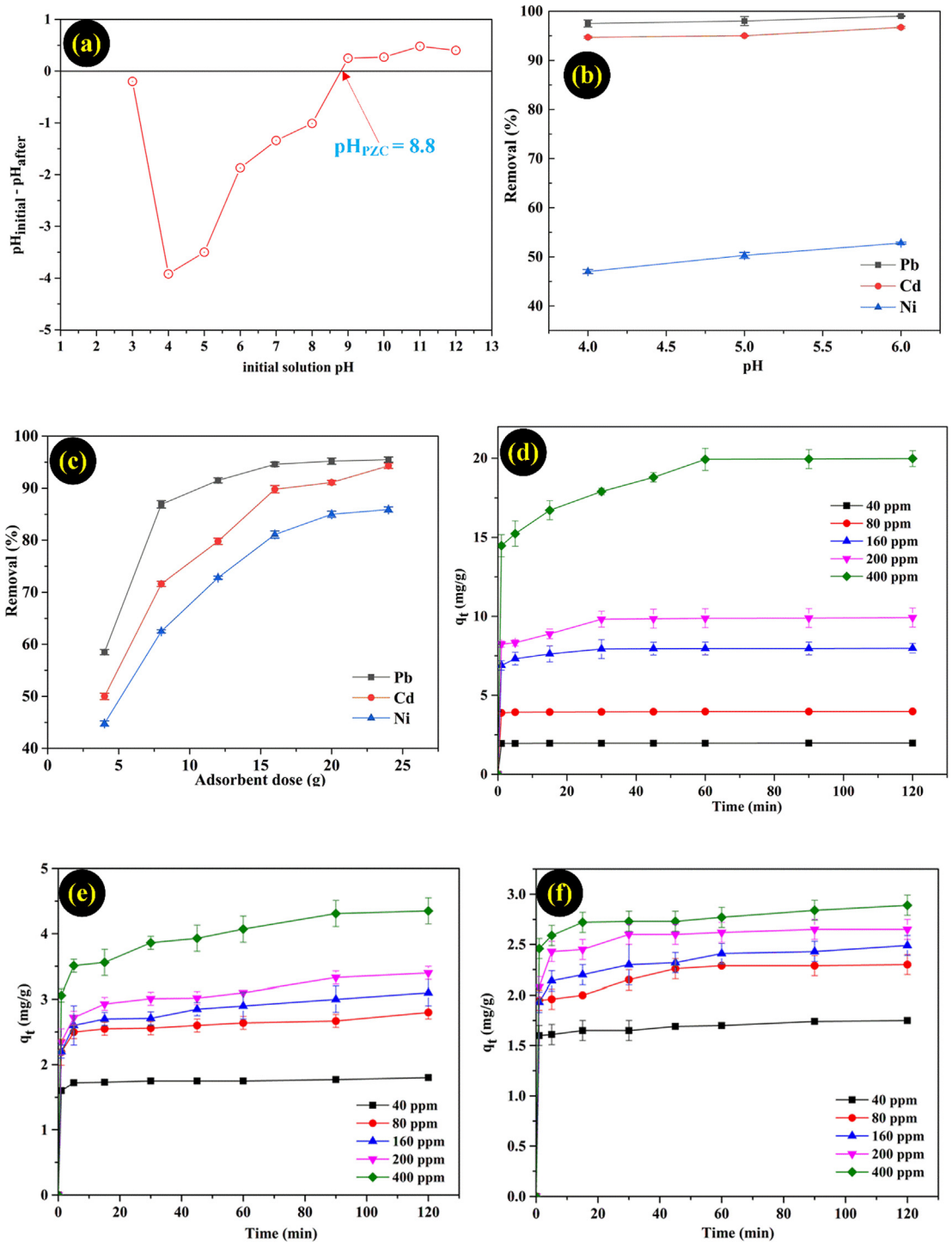

Fig. 4 Effect of pH_{pzc} (a), pH (b), adsorbent dose (c), initial concentration and contact time (d, e, f) of Pb(II), Cd(II), Ni(II).

to 96.7%, and 47% to 52.8%, as the pH value was increased from 4 to 6, respectively. The adsorption data was fitted with the optimum pH value as 5 for all experiments (see Fig. 5).

3.2.2. Effect of MMT/Starch dose

The adsorption capacity of Pb(II), Cd(II), and Ni(II) with various dosage of MMT/Starch were investigated and the results were shown in Fig. 4c. The adsorbent dosage was increased from 4 g/L to 24 g/L and the result showed the highest removal rate of Ni(II) than Pb(II) and Cd(II) ions. As a result, the phenomenon is the present availability of adsorption sites on the surface adsorbent and the best removal for on the adsorbent was fitted all the batch experiment such as 20 g/L of adsorbent dose.

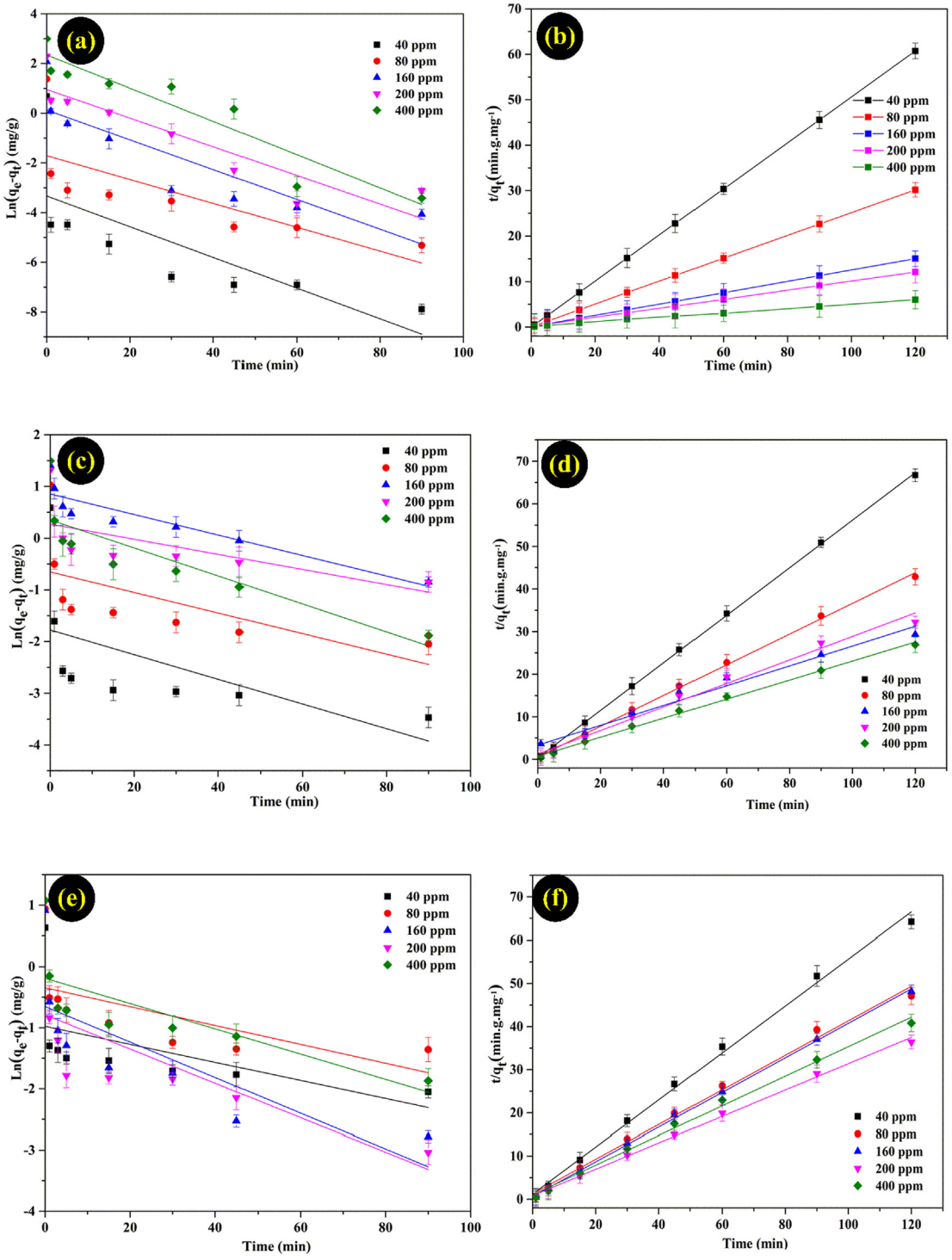

Fig. 5 Pseudo-first-order and Pseudo-second-order models of Pb (II)(a,b), Cd(II)(c,d), and Ni(II)(e,f) ions on MMT/ Starch adsorbent.

3.2.3. Effect of initial concentration and adsorption time

The influence of initial concentration (40–400 mg/L) for the removal of Pb(II), Cd(II), and Ni(II) ion solutions were shown in Fig. 4d–f. The adsorption uptake of metal ions were significantly increased almost 15 min due to a reaction process occurred between the active sites of the adsorbent and metal ions in the solution. Then, the adsorption followed lesser because the presence of function group sites on the surface gradually decreased and adsorption process reached to equilibrium state. In fact, the adsorption uptake increased from 1.98 to 19.95 mg/g for Pb(II) ion, from 1.75 to 4.31 mg/g for Cd(II) ion, and from 1.85 to 2.84 mg/g for Ni(II) ion with an increased in the initial metal ions from 40 to 400 mg/L.

3.3. Adsorption kinetics

The adsorption kineticand the mechanism of MMT/Starch and metal ions were investigated at equilibrium state. The kinetic data of metal ions on adsorbent was studied using four kinetic models: pseudo-first model, pseudo-second order model, Elovich model, and Intra-particle diffusion models which are given in the below following equations (Foo and Hameed, 2010, Tran et al., 2017):

$$\mathrm{Ln}(q_e - q_t) = \mathrm{ln}q_e - k_1 t \quad (2)$$

$$\frac{t}{q_t} = \frac{1}{k_2 q_e^2} + \frac{t}{q_e} \quad (3)$$

Where k_1 and k_2 are the rate constant of pseudo-first-order ($gmg^{-1}min^{-1}$) and pseudo-second-order ($gmg^{-1}min^{-1}$) models; q_t and q_e represent the adsoprtion capacity of metal ions (mg/g) at time t and at equilibrium, respectively. However, the pseudo-first-order kinetic model using $\ln(q_e - q_t)$ against ln(t) and the pseudo second-order kinetic model using t/q_t against (t), are analyzed from the experimental data.

Elovich model is used to determine the heterogeneous reactions on the solid surface. This equation can be followed:

$$q_t = \frac{1}{\beta}\ln(t) + \frac{1}{\beta}\ln(\alpha\beta) \quad (4)$$

Where α and β represent the initial adsorption rate (mgg^{-1} min^{-1}) and the desorption constant (gmg^{-1}), respectively. The plot of q_t versus lnt may be given a linear form with an intercep of β ln(αβ) and a slope of β.

The intra-particle diffusion model is characterized the diffusion capacity of different adsorbates into the structure adsorbents, which is can be followed the below equation:

$$q_t = k_i\sqrt{t} + C \quad (5)$$

Where k_i is intra-particle diffusion rate constant ($mg\ g^{-1}$ $min^{-1/2}$) and C is a constant which indicates the thickness of boundary layer. The k_i and q_t values of this equation is calculated at the curve of q_t versus $t^{1/2}$.

Table 1 Four kinetic models of Pb (II)(a), Cd(II)(b), andNi(II)(c) ions on MMT/Starch adsorbent.

Models	Unit	Heavy metal	C_o (mg/L)				
			40	80	160	200	400
Pseudo-first-order model	Q_e (mg/g)	Pb (II)	0.26	0.32	1.13	2.59	10.43
	K_1 (min^{-1})		0.078	0.057	0.060	0.058	0.067
	R^2		0.843	0.700	0.759	0.831	0.893
Pseudo-second-order model	Q_e (mg/g)		1.98	3.98	8.01	10.00	20.40
	K_2 (g/mg min^{-1})		1.65	2.13	0.32	0.09	0.02
	R^2		1.000	1.000	1.000	0.999	0.998
Elovich model	α mg/(g × min)		9.53E + 17	1.93E + 94	8.14E + 11	67.57E + 6	49.86E + 3
	β (mg/g)		24.691	56.818	4.149	2.365	0.769
	R^2		0.910	0.968	0.948	0.906	0.905
Intra-particle diffusion model	k_i mg/(g × $min^{1/2}$)		0.001	0.008	0.099	0.193	0.614
	C (mg/g)		1.965	3.901	7.109	8.159	14.122
	R^2		0.808	0.840	0.746	0.865	0.927
Pseudo-first-order model	Q_e (mg/g)	Cd (II)	0.32	1.51	2.69	2.97	3.03
	K_1 (min^{-1})		0.027	0.016	0.020	0.015	0.031
	R^2		0.444	0.601	0.891	0.852	0.785
Pseudo-second-order model	Q_e (mg/g)		1.79	2.77	3.90	3.97	5.18
	K_2 (g/mg min^{-1})		0.89	0.22	0.03	0.03	0.03
	R^2		0.999	0.999	0.982	0.957	0.980
Elovich model	α mg/(g × min)		2.07E + 19	23.17E + 7	7.962	53.68E + 2	8.170
	β (mg/g)		29.411	9.606	2.094	4.365	0.365
	R^2		0.868	0.914	0.896	0.856	0.94
Intra-particle diffusion model	k_i mg/(g × $min^{1/2}$)		0.008	0.031	0.209	0.097	0.115
	C (mg/g)		1.701	2.411	1.634	2.467	3.196
	R^2		0.900	0.919	0.960	0.871	0.984
Pseudo-first-order model	Q_e (mg/g)	Ni (II)	0.44	0.65	0.680	0.72	0.999
	K_1 (min^{-1})		0.016	0.056	0.031	0.033	0.022
	R^2		0.400	0.885	0.735	0.674	0.657
Pseudo-second-order model	Q_e (mg/g)		1.84	2.32	2.50	3.51	3.83
	K_2 (g/mg min^{-1})		0.24	0.35	0.24	0.03	0.02
	R^2		0.997	0.999	0.989	0.985	0.983
Elovich model	α mg/(g × min)		1.56E + 22	16.03E + 7	71.77E + 5	2.78E + 12	11.51E + 5
	β (mg/g)		34.602	11.325	9.285	12.658	7.541
	R^2		0.861	0.869	0.978	0.961	0.925
Intra-particle diffusion model	k_i mg/(g × $min^{1/2}$)		0.016	0.048	0.054	0.039	0.067
	C (mg/g)		1.578	1.885	1.967	2.487	2.152
	R^2		0.981	0.944	0.903	0.861	0.852

In this investigation, four adsorption kinetic models were compared the adsorption process of Pb(II), Cd(II), and Ni (II) ions on MMT/Starch adsorbent (Table 1). Moreover, the experimental results on four adsorption models showed that pseudo-second-order model was well fitted with the correlation coefficient was higher (R^2 > 0.99) than pseudo-first-order, Elovich, and Intra-particle diffusion models. According to the intial concentration in range of 40–400 (mg/L), the Q_e values of Pb(II) ion in pseudo-second-order model were sharply increased from 1.98 to 20.4 (mg/g). On the other hand, the Q_e values of Cd(II) and Ni(II) ions were lower than 4 (mg/g) from 40 to 400 (mg/L). In general, the phenomenon of MMT/Starch in equilibrium was reached a high adsorption for Pb(II) ion.

3.4. Equilibrium adsorption isotherm

To study the interaction relationship between metal ions in the solution and the amount of adsorbent at equilibrium, four adsorption isotherms were investigated Sips, Redlich-Peterson, Langmuir and Freundlich isotherm models (Ayawei et al., 2017, Zhu et al., 2014). The adsorption capacity on the adsorbent was studied at initial metal ion concentration of the range from 40 to 400 mg/L at room temperature, and the shaking speed of 150 rpm (Fig. 6).

The adsorption isotherm equations are given by the following equations, respectively:

$$\frac{C_e}{q_e} = \frac{C_e}{q_m} + \frac{1}{K_L q_m} \tag{6}$$

$$\ln q_e = \ln K_F + \frac{1}{n}\ln C_e \tag{7}$$

Where C_e (mg/L) and q_e (mg/g) represents the metal ions concentration and the amount of adsorbent at equilibrium time, respectively; andq_m (mg/g) is the maximum adsorption capacity; K_L is Langmuir constant (L/mg); K_F (L/mg) is the Freundlich adsorption contant for the interaction process of adsorbent and adsorbate; and n is the heterogeneity factor.

Redlich-Peterson model combines the characteristics of Langmuir and Freundlich models for applying various absorbates in a range of wide concentrations. This model is a nonlinear form is indicated as follows:

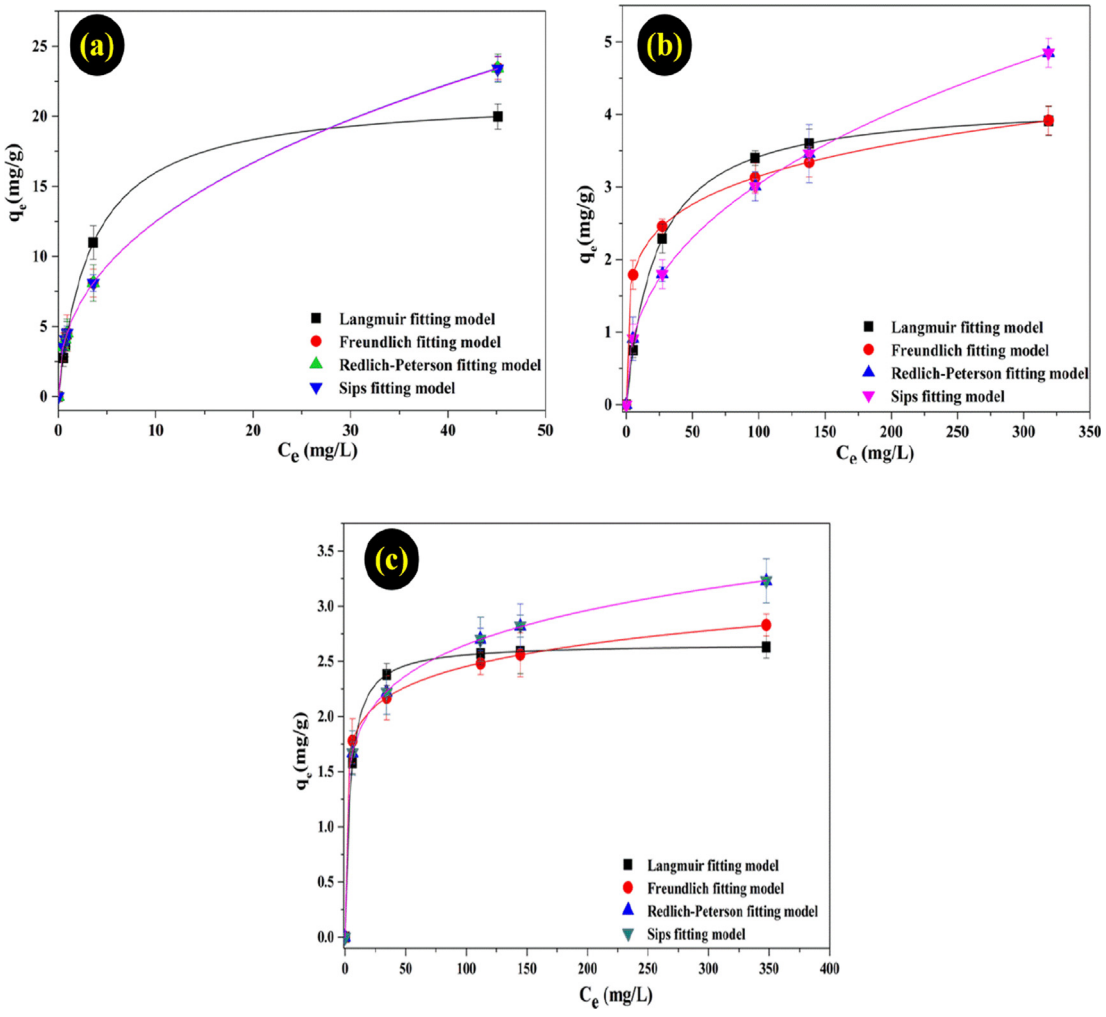

Fig. 6 Adsorption equilibrium data of Pb (II), Cd(II), and Ni(II) ions on MMT/Starch from aqueous solution fitting to Langmuir, Freundlich, Redlich-Peterson, Sips isotherm models.

$$q_e = \frac{K_{RP}C_e}{1 + a_{RP}C_e^g} \quad (8)$$

Where a_{RP} (mg/L) and K_{RP} (L/g) are Redlich-Peterson constants and g is an exponent that this value is between 0 and 1, C_e is equilibrium concentration of adsorbent, and q_e is the capacity of adsorbent at equilibrium (mg/g)

Sips model incorporates the properties of Freundlich and Langmuir models and it is explained the following equation:

$$q_e = \frac{Q_s C_e^{\beta_s}}{1 + \alpha_s C_e^{\beta_s}} \quad (9)$$

Where Q_s and α_s are Sips constant (L/g), β_s is Sips model exponent. β_s is a parameter explaining the characteristics of homogeneous/heterogeneous of the adsorption process. For $0 < \beta_s < 1$, the adsorption occurs heterogeneous phenomenon at multi-site adsorption. For $\beta_s = 1$, the adsorption is homogeneous phenomenon and Sips isotherm model shift to the Langmuir model. For $\beta_s > 1$, the adsorption process take place the adsorbate formation with multi-layer on the material surface.

In this investigation, four adsorption isotherms (Langmuir, Redlich- Peterson, and Sips models) were applied to describe the adsorption behaviour of MMT/Starch at equilibrium. The fitting isotherm models were indicated in Fig. 6. In addition, the detail results were presented in Table 2 and the experimental data of adsorbent were well fitted the Langmuir model than the Freundlich, Redlich-Peterson, and Sips models. The curves of graph are suitable for the experimental values that are described in Fig. 6. Overall, the maximum adsorption capacity for Langmuir isotherm exhibited the decreased values: Pb(II) 21.5 (mg/g) > Cd(II) (4.2 mg/g) > Ni(II) (2.7 mg/g).

For various adsorbent at different conditions, the removal capacity of Pb(II), Cd(II), and Ni(II) ions are compared other studies and the experimental results are indicated in Table 3. The Pb(II) adsorption capacity of MMT/Starch is better at the removing uptake than most of adsorbents in aqueous solution. On the other hand, the removal of Cd(II) and Ni(II) ions are lower than other adsorbents. Furthermore, MMT/Starch adsorbent has been found maximun adsorption uptake of Pb (II) ion than the adsorption process of Cd(II) and Ni(II) ions

3.5. Discussion on adsorption mechanism

In order to determine the interaction mechanism between metal ions and MMT/Starch. the electrostatic attraction between these ions and permanent negatively charged moieties

Table 2 Parameters of Langmuir, Freundlich, Redlich-Peterson, Sips models for the adsorption of Pb (II), Cd(II), and Ni(II) ions on MMT/Starch adsorbent.

Isotherm fitting models		Element metal		
		Pb(II)	Cd(II)	Ni(II)
Langmuir	Q_m(mg/g)	21.5	4.2	2.7
	b (L/mg)	0.007	1.293	0.581
	R^2	0.996	0.990	0.998
Freundlich	N	2.38	5.30	8.77
	K_f(L/mg)	4.73	1.32	1.45
	R^2	0.767	0.968	0.785
Redlich-Peterson	g	0.580	0.596	0.835
	a_{RP} (mg/L-g)	0.859	0.812	0.911
	K_{RF} (L/g)	16.035	6.719	8.613
	R^2	0.769	0.917	0.927
Sips	β_s	0.420	0.404	0.165
	α_s	0.988	0.137	0.032
	Q_s	4,599	0.478	1.319
	R^2	0.769	0.917	0.927

Table 3 The effect of adsorption uptake of Pb(II), Cd(II), and Ni(II) ions on different adsorbents.

Adsorbents	Q_{max}			pH	Refs
	Pb(II) (mg/g)	Cd (II) (mg/g)	Ni(II) (mg/g)		
Activated bentonite	21.36	–	–	5	(Pawar et al., 2016)
Ca-montmorillonite	–	–	5.969	4	(de Pablo et al., 2011)
Montmorillonite from binodal Metal + Ca^{2+} solution	–	6.978	4.849	4.8	(Kumrić et al., 2013)
Montmorillonite	9.58	–	–	5.5	(Abollino et al., 2008)
Na-MMT	7.52	–	–	3.6	(Heiba et al., 2017)
Ca-MMT	–	1.53	–	–	(Abdellaoui et al., 2019)
Amino magnetic nanoparticles coated montmorillonite	38.15	–	–	6.5	(Irawan et al., 2019)
MMT/Starch	21.5	4.2	2.7	5	This study

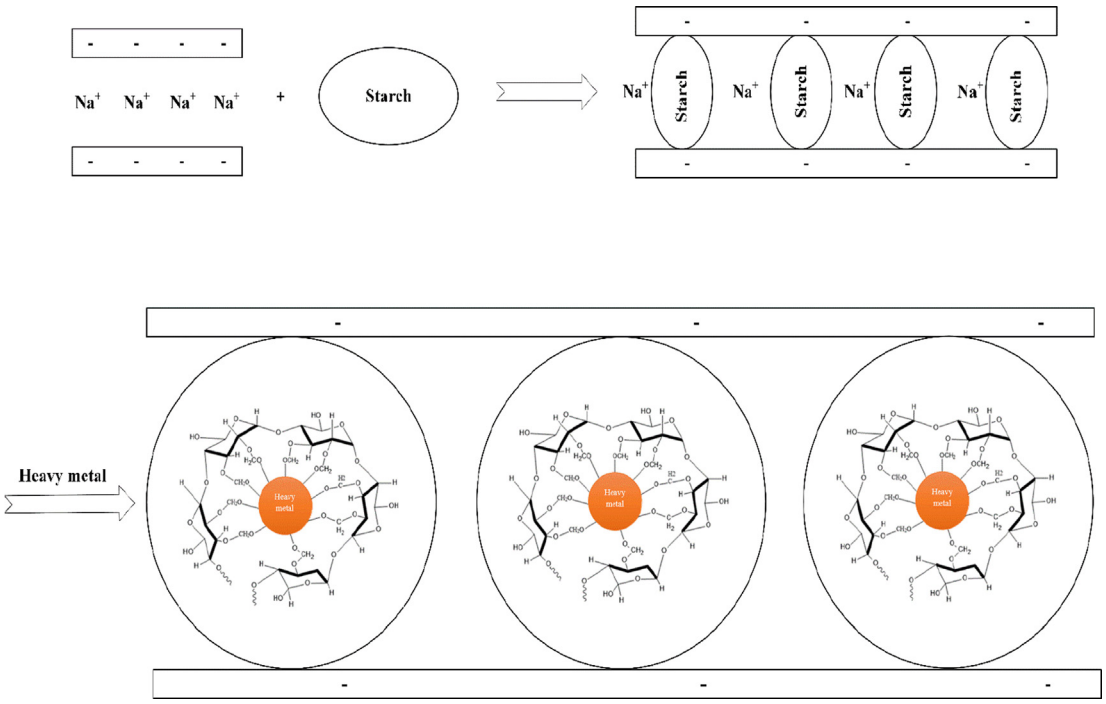

Fig. 7 Possible mechanism adsorption of MMT modified Starch.

of the adsorbent, and the chemical binding between polar functional groups, like hydroxyls, on the surface of the adsorbent, and metal ions are described the main role. The former binding is indicated a process of specific adsorption, which is played less reversible and more selective reactions. The study of heavy metals adsorption by MMT has been reported before in literature (Abollino et al., 2008, de Pablo et al., 2011, Kumrić et al., 2013, Abdellaoui et al., 2019) and the preparation of MMT intercalated by cassava starch molecules from natural source, which has not been reported before, expected bringing more interesting efficient adsorption property for heavy metals treatment. Based on the theory showing that the ionic heavy metal may bind to the OH group of starch molecules to form the stable ionic complexes in water environment, so the potential modified MMT by starch in having the larger clay gallery and starch molecules inside, should be expected to enhance the adsorption capacity of neat MMT. That's why the main objective of this study was to valorize the Vietnamese abundant agroindustrial vegetable starch and natural MMT for the obtaining of value-added of adsorbent which is being attracted as a potential material for water treatment at room temperature, and the shaking speed of 150 rpm (Fig. 7).

4. Conclusion

In this study, MMT/Starch was prepared by mixing the solutions of MMT and starch. A new adsorbent was an effective low-cost for the removal of Pb(II), Cd(II), and Ni(II) ions from aqueous solutions. Besides, the characteristics of MMT/Starch adsorbent were investigated at the various conditions: pH, dose, initial metal ion concetration and contact time. Furthermore, the equilibrium adsorption data were fitted well the Langmuir isotherm model in comparison to Freundlich, Redlich-Peterson, and Sips isotherm model. In addition, the pseudo-second-order kinetic model was better than the pseudo-first-order model, Intra-particle diffusion, and Elovich models, which are given the process of chemical adsorption rather than the diffusion in adsorbent-adsorbate system. As a result, the maximum adsorption capacity was determined as 21.5 mg/g for Pb(II), for 4.2 mg/g Cd(II) and 2.7 mg/g for Ni(II), respectively. The adsorption mechanism for metal ions was chemisorption on MMT/Starch as alternative adsorbent for removing metal ions from aqueous solution.

Declaration of Competing Interest

The authors declare that they have no known competing financial interests or personal relationships that could have appeared to influence the work reported in this paper.

References

Abdellaoui, Y., Olguín, M.T., Abatal, M., Ali, B., Díaz Méndez, S.E., Santiago, A.A., 2019. Comparison of the divalent heavy metals (Pb, Cu and Cd) adsorption behavior by montmorillonite-KSF and their calcium- and sodium-forms. Superlattices Microstruct. 127, 165–175.

Abollino, O., Giacomino, A., Malandrino, M., Mentasti, E., 2008. Interaction of metal ions with montmorillonite and vermiculite. Appl. Clay Sci. 38, 227–236.

Achazhiyath Edathil, A., Shittu, I., Hisham Zain, J., Banat, F., Abu Haija, M., 2018. Novel magnetic coffee waste nanocomposite as effective bioadsorbent for Pb(II) removal from aqueous solutions. Journal of Environmental. Chem. Eng. 6.

Akpomie, K.G., Dawodu, F.A., 2016. Acid-modified montmorillonite for sorption of heavy metals from automobile effluent. Beni-Suef Univ. J. Basic Appl. Sci. 5, 1–12.

Ayawei, N., Ebelegi, A.N., Wankasi, D., 2017. Modelling and Interpretation of Adsorption Isotherms. J. Chem. 2017, 3039817.
Bo, S., Ren, W., Lei, C., Xie, Y., Cai, Y., Wang, S., Gao, J., Ni, Q., Yao, J., 2018. Flexible and porous cellulose aerogels/zeolitic imidazolate framework (ZIF-8) hybrids for adsorption removal of Cr(IV) from water. J. Solid State Chem. 262, 135–141.
Chuah, T.G., Jumasiah, A., Azni, I., Katayon, S., Thomas Choong, S. Y., 2005. Rice husk as a potentially low-cost biosorbent for heavy metal and dye removal: an overview. Desalination 175, 305–316.
Dai, R., Zhang, Y., Shi, Z.-Q., Yang, F., Zhao, C.-S., 2018. A facile approach towards amino-coated ferroferric oxide nanoparticles for environmental pollutant removal. J. Colloid Interface Sci. 513, 647–657.
Dardouri, M., Ammari, F., Amor, A., Meganem, F., 2018. Adsorption of cadmium (II), zinc (II) and iron (III) from water by new cross-linked reusable polystyrene adsorbents. Mater. Chem. Phys. 216.
de Pablo, L., Chávez, M.L., Abatal, M., 2011. Adsorption of heavy metals in acid to alkaline environments by montmorillonite and Ca-montmorillonite. Chem. Eng. J. 171, 1276–1286.
Dimpe, K.M., Ngila, J.C., Nomngongo, P.N., 2018. Preparation and application of a tyre-based activated carbon solid phase extraction of heavy metals in wastewater samples. Phys. Chem. Earth, Parts A/B/C 105, 161–169.
Dong, C., Zhang, F., Pang, Z., Yang, G., 2016. Efficient and Selective Adsorption of Multi-metal Ions Using Sulfonated Cellulose as Adsorbent. Carbohydr. Polym. 151.
Eeshwarasinghe, D., Loganathan, P., Vigneswaran, S., 2019. Simultaneous removal of polycyclic aromatic hydrocarbons and heavy metals from water using granular activated carbon. Chemosphere 223, 616–627.
Fakhre, N.A., Ibrahim, B.M., 2018. The use of new chemically modified cellulose for heavy metal ion adsorption. J. Hazard. Mater. 343, 324–331.
Foo, K.Y., Hameed, B.H., 2010. Insights into the modeling of adsorption isotherm systems. Chem. Eng. J. 156, 2–10.
Heiba, H., Shreadah, M., Taha, A.A., 2017. Validity of Egyptian Na-Montmorillonite for adsorption of Pb^{2+}, Cd^{2+} and Ni^{2+} under acidic conditions: Characterization, Isotherm, kinetics, thermodynamics, and application study. Asia-Pac. J. Chem. Eng. 12, 292–306.
Hu, Z.-H., Omer, A., Ouyang, X.K., Yu, D., 2018. Fabrication of carboxylated cellulose nanocrystal/sodium alginate hydrogel beads for adsorption of Pb(II) from aqueous solution. Int. J. Biol. Macromol. 108, 149–157.
Huang, R., Lin, Q., Zhong, Q., Zhang, X., Wen, X., Luo, H., 2020. Removal of Cd(II) and Pb(II) from aqueous solution by modified attapulgite clay. Arabian J. Chem. 13, 4994–5008.
Irawan, C., Nata, I.F., Lee, C.-K., 2019. Removal of Pb(II) and As(V) using magnetic nanoparticles coated montmorillonite via one-pot solvothermal reaction as adsorbent. J. Environ. Chem. Eng. 7, 103000.
Karri, R.R., Sahu, J.N., Meikap, B.C., 2020. Improving efficacy of Cr (VI) adsorption process on sustainable adsorbent derived from waste biomass (sugarcane bagasse) with help of ant colony optimization. Ind. Crops Prod. 143, 111927.
Kenawy, I.M., Hafez, M.A.H., Ismail, M., Hashem, M.A., 2017. Adsorption of Cu(II), Cd(II), Hg(II), Pb(II) and Zn(II) from aqueous single metal solutions by guanyl-modified cellulose. Int. J. Biol. Macromol., 107
Kumrić, K.R., Đukić, A.B., Trtić-Petrović, T.M., Vukelić, N.S., Stojanović, Z., Grbović Novaković, J.D., Matović, L.L., 2013. Simultaneous removal of divalent heavy metals from aqueous solutions using raw and mechanochemically treated interstratified montmorillonite/kaolinite clay. Ind. Eng. Chem. Res. 52, 7930–7939.
Li, C., Zhang, M., Zhong, H., He, H., Feng, Y., Yin, X., 2018. Synthesis of a bioadsorbent from jute cellulose, and application for aqueous Cd (II) removal. Carbohydr. Polym. 189, 152–161.
Li, Y., Bai, P., Yan, Y., Yan, W., Shi, W., Xu, R., 2019. Removal of Zn^{2+}, Pb^{2+}, Cd^{2+}, and Cu^{2+} from aqueous solution by synthetic clinoptilolite. Micropor. Mesopor. Mater. 273, 203–211.
Lozano-Morales, V., Gardi, I., Nir, S., Undabeytia, T., 2018. Removal of pharmaceuticals from water by clay-cationic starch sorbents. J. Cleaner Prod. 190, 703–711.
Luo, X., Zeng, J., Liu, S., Zhang, L., 2015. An effective and recyclable adsorbent for the removal of heavy metal ions from aqueous system: Magnetic chitosan/cellulose microspheres. Bioresour. Technol. 194, 403–406.
Majdzadeh-Ardakani, K., Navarchian, A.H., Sadeghi, F., 2010. Optimization of mechanical properties of thermoplastic starch/clay nanocomposites. Carbohydr. Polym. 79, 547–554.
Kosmulski, Marek, 2009. pH-dependent surface charging and points of zero charge. IV. Update and new approach. Journal of Colloid and Interface Science. 337 (2), 439–448.
Masoumi, A., Hemmati, K., Ghaemy, M., 2016. Low-cost nanoparticles sorbent from modified rice husk and a copolymer for efficient removal of Pb(II) and crystal violet from water. Chemosphere 146, 253–262.
Mende, M., Schwarz, D., Steinbach, C., Boldt, R., Schwarz, S., 2016. Simultaneous adsorption of heavy metal ions and anions from aqueous solutions on chitosan—Investigated by spectrophotometry and SEM-EDX analysis. Colloids Surf., A 510, 275–282.
Mousavi, S.J., Parvini, M., Ghorbani, M., 2018. Adsorption of heavy metals (Cu^{2+} and Zn^{2+}) on novel bifunctional ordered mesoporous silica: Optimization by response surface methodology. J. Taiwan Inst. Chem. Eng. 84, 123–141.
Namasivayam, C., Sangeetha, D., 2006. Recycling of agricultural solid waste, coir pith: Removal of anions, heavy metals, organics and dyes from water by adsorption onto ZnCl2 activated coir pith carbon. J. Hazard. Mater. 135, 449–452.
Oninla, V.O., Olatunde, A.M., Babalola, J.O., Adesanmi, O.J., Towolawi, G.S., Awokoya, K.N., 2018. Qualitative assessments of the biomass from oil palm calyxes and its application in heavy metals removal from polluted water. J. Environ. Chem. Eng. 6, 4044–4053.
Pawar, R.R., Lalhmunsiama, Bajaj, H.C., Lee, S.-M., 2016. Activated bentonite as a low-cost adsorbent for the removal of Cu(II) and Pb (II) from aqueous solutions: Batch and column studies. J. Ind. Eng. Chem. 34, 213–223.
Rathinam, K., Singh, S.P., Arnusch, C.J., Kasher, R., 2018. An environmentally-friendly chitosan-lysozyme biocomposite for the effective removal of dyes and heavy metals from aqueous solutions. Carbohydr. Polym. 199, 506–515.
Rytwo, G., Kohavi, Y., Botnick, I., Gonen, Y., 2007. Use of CV- and TPP-montmorillonite for the removal of priority pollutants from water. Appl. Clay Sci. 36, 182–190.
Sandoval, O.G.M., Trujillo, G.C.D., Orozco, A.E.L., 2018. Amorphous silica waste from a geothermal central as an adsorption agent of heavy metal ions for the regeneration of industrial pretreated wastewater. Water Resour. Ind. 20, 15–22.
Sellaoui, L., Soetaredjo, F.E., Ismadji, S., Bonilla-Petriciolet, A., Belver, C., Bedia, J., Ben Lamine, A., Erto, A., 2018. Insights on the statistical physics modeling of the adsorption of Cd^{2+} and Pb^{2+} ions on bentonite-chitosan composite in single and binary systems. Chem. Eng. J. 354, 569–576.
Semerjian, L., 2018. Removal of heavy metals (Cu, Pb) from aqueous solutions using pine (Pinus halepensis) sawdust: Equilibrium, kinetic, and thermodynamic studies. Environ. Technol. Innovat., 12
Sun, N., Wen, X., Yan, C., 2018. Adsorption of mercury ions from wastewater aqueous solution by amide functionalized cellulose from sugarcane bagasse. Int. J. Biol. Macromol. 108, 1199–1206.
Tam, L.H., Hung, N.V., 2019. Synthesis of starch modified montmorillonite as an effective adsorbent for Pb (II) removal from water. Vietnam J. Sci. Technol. 57, 94–102.

Tang, X., Zhang, Q., Liu, Z., Pan, K., Dong, Y., Li, Y., 2014. Removal of Cu(II) by loofah fibers as a natural and low-cost adsorbent from aqueous solutions. J. Mol. Liq. 191, 73–78.

Thuc, C.-N.H., Grillet, A.-C., Reinert, L., Ohashi, F., Thuc, H.H., Duclaux, L., 2010. Separation and purification of montmorillonite and polyethylene oxide modified montmorillonite from Vietnamese bentonites. Appl. Clay Sci. 49, 229–238.

Tian, Y., Wu, M., Liu, R., Li, Y., Wang, D., Tan, J., Wu, R., Huang, Y., 2011. Electrospun membrane of cellulose acetate for heavy metal ion adsorption in water treatment. Carbohydr. Polym. 83, 743–748.

Tohdee, K., Kaewsichan, L., Asadullah, 2018. Enhancement of adsorption efficiency of heavy metal Cu(II) and Zn(II) onto cationic surfactant modified bentonite. J. Environ. Chem. Eng. 6, 2821–2828.

Tran, H.N., You, S.-J., Hosseini-Bandegharaei, A., Chao, H.-P., 2017. Mistakes and inconsistencies regarding adsorption of contaminants from aqueous solutions: A critical review. Water Res. 120, 88–116.

Zhu, W., Liu, J., Li, M., 2014. Fundamental studies of novel zwitterionic hybrid membranes: kinetic model and mechanism insights into strontium removal. Sci. World J. 2014, 485820.